frontiers | Frontiers in Environmental Chemistry

TYPE Original Research
PUBLISHED 12 June 2025
DOI 10.3389/fenvc.2025.1581103

Check for updates

OPEN ACCESS

EDITED BY
Si Chen,
Argonne National Laboratory (DOE),
United States

REVIEWED BY
Shiue-Lin Li,
Tunghai University, Taiwan
Kledi Xhaxhiu,
University of Tirana, Albania

*CORRESPONDENCE
Tetyana Milojevic,
tetyana.milojevic@cnrs-orleans.fr

†PRESENT ADDRESSES
Mihaela Albu,
The Austrian Research Promotion Agency,
Vienna, Austria

RECEIVED 21 February 2025
ACCEPTED 28 May 2025
PUBLISHED 12 June 2025

CITATION
Milojevic T, Albu M, Letofsky-Papst I and Mashchenko A (2025) Nanoscale investigations of complex microbial interactions with terrestrial and extraterrestrial minerals using STEM based approach: implications for life on Earth and beyond.
Front. Environ. Chem. 6:1581103.
doi: 10.3389/fenvc.2025.1581103

COPYRIGHT
© 2025 Milojevic, Albu, Letofsky-Papst and Mashchenko. This is an open-access article distributed under the terms of the Creative Commons Attribution License (CC BY). The use, distribution or reproduction in other forums is permitted, provided the original author(s) and the copyright owner(s) are credited and that the original publication in this journal is cited, in accordance with accepted academic practice. No use, distribution or reproduction is permitted which does not comply with these terms.

Nanoscale investigations of complex microbial interactions with terrestrial and extraterrestrial minerals using STEM based approach: implications for life on Earth and beyond

Tetyana Milojevic[1]*, Mihaela Albu[2†], Ilse Letofsky-Papst[2] and Artem Mashchenko[1]

[1]Exobiology Group, CNRS-Centre de Biophysique Moléculaire, University of Orléans, Orléans, France, [2]Institute of Electron Microscopy and Nanoanalysis and Centre for Electron Microscopy, Graz University of Technology, Graz, Austria

Our recent investigations using scanning transmission electron microscopy (STEM) based approach address tungsten-microbial interactions as a microbial strategy to withstand harsh environments, microbial metal extraction capacities for bioleaching/biomining operations, astrobiological implication of microbial-mineral interactions, and Mars-relevant biosignatures as traces of life that can be detected in the physicochemical conditions beyond Earth. By means of STEM based nanoscale resolution ultrastructural studies coupled to energy dispersive spectroscopy (EDS) and electron energy loss spectroscopy (EELS), we have investigated remarkable metal redox events and unique ultrastructural features of the mineral-microbial interfaces with regard to the mechanisms of mineral biotransformation mediated by various chemolithoautotrophs; the subcellular localization of metal incorporation and binding sites; the chemical nature of the metal complexes formed at the microbe-mineral interfaces; and biomineral patterns formed during the biotransformation of terrestrial minerals and astromaterials. Our results indicate that microbial cells form a robust, metal-bearing cell crust that may help microorganisms withstand harsh environments and serve as potential biosignature for the search of life. During the biomineralization of the microbial cell surface with tungsten, a tungsten-encrusted layer with a thickness of 37 $\pm$ 7 nm and a W content of 76.3% (Wt) was formed around the *Metallosphaera sedula* cells. When cultivated on the genuine Noachian Martian breccia Northwest Africa (NWA) 7,034, *M. sedula* cells were encrusted in a mineral layer of 28 $\pm$ 2 nm thickness and a P, Fe, Mn, and Al content of 9.62% (Wt), 11.65% (Wt), 4.29% (Wt), and 2.82% (Wt), respectively. During these investigations, we have developed an efficient combined approach of microbiology, wet chemistry and STEM based spectroscopy nanoanalysis. This work highlights the biologically-mediated processing of (extra) terrestrial materials, provides implications for natural samples and biotechnological processes, and represents a special interest for space exploration missions.

KEYWORDS

chemolithoautotrophs, microbial-mineral interactions, transmission scanning electron microscopy, EDS, EELS, Mars and meteorites

1 Introduction

Microorganisms accelerate rocks transformation, promote mineral weathering, influence sedimentary processes and diagenesis, and ubiquitously solubilise and produce various minerals, impacting the lithosphere in diverse and significant ways. The mechanisms in which microorganisms perform rock-transforming processes are one of the most vital geological and biological questions. Understanding the mineral-microbial interactions extends our knowledge of the processes on early Earth, early life forms and their biosignatures, facilitates the search of life beyond Earth, and advances such industrial biotechnologies as sustainable metal recovery and "green" recycling of planetary resources (Krebs et al., 1997; Giachino et al., 2021; Pham et al., 2022).

Some of metal- and mineral-transforming microorganisms are the ancient metabolic forms of life that thought to have enabled the transition of geochemistry into geobiochemistry and served as a biochemical link between the mineral world and the last universal common ancestor (LUCA) (Weiss et al., 2016; Camprubi et al., 2017; Wächtershäuser, 1988; Wächtershäuser, 1990). Such metal-loving microorganisms employ an astonishing number of metabolic pathways to extract energy from various inorganic electron donors and acceptors (Claassens, 2016), forming global geobiochemical cycles. Flourishing in hot acid enriched with heavy metals, these microbes learned to extract energy from sources that are inaccessible to other life forms (Auernik et al., 2008) at temperatures ranging from 40°C to 95°C and pH levels between 1 and 6. Such microorganisms (chemolithoautotrophs) thrive in geothermal environments (Huber et al., 1989; Yoshida et al., 2006) and metabolise inorganic chemicals, a source of energy that, on the one hand, provided the most likely habitable niches for life on early Earth and Mars (Grotzinger et al., 2014; Hurowitz et al., 2017; Bristow, 2015; Vaniman et al., 2014; Farquhar et al., 2000; Weiss et al., 2016; Morrison and Mojzsis, 2020) and on the other hand, fuelled the metal solubilising capacities of these microorganisms needed for bioleaching/biomining operations (Bosecker, 1997; Schippers et al., 2013; Banerjee et al., 2017). Acidophilic chemolithotrophs have also been suggested to influence terrestrial geobiochemistry in iron-rich sedimentary rocks during the Great Oxidation Event (Konhauser et al., 2011). Driving mineral evolution at the global scale, mineral–microbe interactions typically occur at nano- and microscopic scales. Recent technological advances in scanning transmission electron microscopy (STEM) have enabled high resolution nanoscale cell imaging, leading to a direct visualization of microbial cell-mineral interactions. Furthermore, STEM coupled to various nanospectroscopy techniques with enhanced spatial resolution can be used to record microbial micro- and nano-structures and reveal unprecedented events at the microbial-mineral interface, thereby solving exciting geobiological questions. The vigorous ability of rock-transforming microorganisms to colonise mineral matrixes and their mineral-microbial interfaces can be efficiently resolved via a comprehensive geomicrobiological toolbox comprised of high resolution STEM (HR-STEM) coupled to nanoanalytical spectroscopy techniques (Blazevic et al., 2019; Milojevic et al., 2019a; Milojevic et al., 2019b; Milojevic et al., 2021; Kölbl et al., 2022). By means of STEM based nanoscale resolution ultrastructural studies coupled to energy dispersive spectroscopy (EDS) and electron energy loss spectroscopy (EELS), remarkable metal redox events and unique ultrastructural features of the mineral-microbial interfaces can be investigated with regard to the mechanisms of mineral biotransformation mediated by various chemolithoautotrophs; the subcellular localization of metal incorporation and binding sites; the chemical nature of the metal complexes formed at the microbe-mineral interfaces; and biomineral patterns formed during the biotransformation of terrestrial minerals and astromaterials. For instances, rare microbial-tungsten interactions have been resolved at the nanometer range using HR-STEM based approach (Blazevic et al., 2019; Milojevic et al., 2019b). A hard metal tungsten with its extraordinary properties and highest melting point of all metals (a boiling point of 5,930°C, diamond-like hardness in combination with carbon) is a very rare choice for a microbiological system. Exceptionally, very few microorganisms (thermophilic archaea) have found a way to accommodate tungsten for their metabolic needs (Milojevic, 2022). In this case, STEM combined with nanoanalytical spectroscopy techniques helps elucidate the possible role of microbes in tungsten-enriched environments.

The presented STEM imaging and nanospectroscopy workflow (Figure 1) enables the characterisation of the microbial-mineral interfaces at the micrometer and nanometer scale, reaching atomic resolution in case with heavy elements. Chemolithotrophic microorganisms are cultivated on various mineral materials in glass bioreactors supplemented with CO_2-gassing under the controlled temperature and pH parameters. Upon harvesting, microbial cells are fixed and their thin sections bearing microbial-mineral interfaces are prepared via ultramicrotome-based and a focused ion beam (FIB) techniques. Subsequently, thin sections are examined in the transmission electron microscopy, whereby element distribution images can be displayed in TEM mode via energy-filtered transmission electron microscopy (EFTEM) method or in STEM mode of the microscope by acquisition of EDS and EELS spectrum images, *i.e.*, also two-dimensional element distributions. Following the elemental analysis, the microbial cells and the cell-associated mineral assemblages can be analysed in high resolution. If particles are crystalline, fast fourier transformation (FFT) patterns can be calculated (Figure 1). The lattice spacings d measured from the FFTs are compared with tabulated values, allowing the corresponding mineral phases to be identified. This workflow enables high resolution surface imaging of microbial-mineral cellular assemblages, tracing the traffic of mineral compounds into microbial cells, and understanding the mechanisms of microbially mediated mineral transformation, thereby delivering important insights for life on Earth and beyond it.

2 Methods and materials

2.1 Cultivation

The extreme thermoacidophilic members of Sulfolobales were cultivated in DSMZ88 Sulfolobus medium consisting of 1.3 g $(NH4)_2SO_4$, 0.28 g KH_2PO_4, 0.25 g $MgSO_4{\cdot}7H_2O$, 0.07 g $CaCl_2{\cdot}2H_2O$, and 0.02 g $FeCl_3{\cdot}6H_2O$ dissolved in 1 L of water. Allen's trace elements solution was added to 1 L media with the total

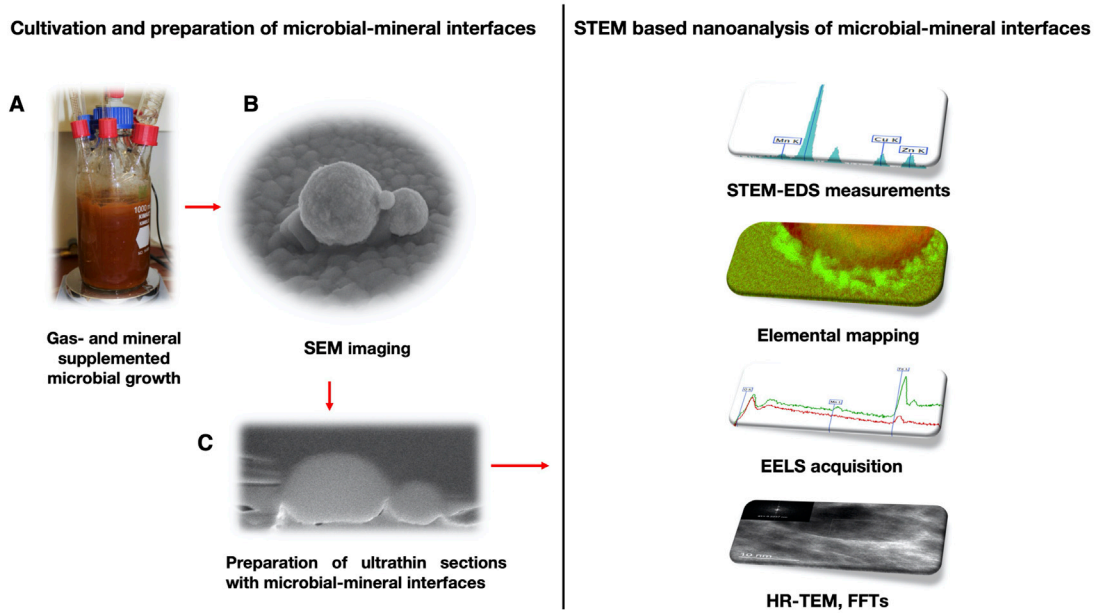

FIGURE 1
Scheme of a STEM based imaging and nanospectroscopy workflow for the characterisation of the microbial-mineral interfaces at the micrometer and nanometer scale. Chemolithotrophic microorganisms are grown on various minerals in glass bioreactors **(A)** supplemented with CO_2-gassing. After harvesting, microbial cells are fixed, examined via Scanning Electron Microscopy (SEM) **(B)** and their thin sections with microbial-mineral interfaces are prepared via ultramicrotome-based or focused ion beam (FIB) techniques **(C)**. Subsequently, thin sections are analysed for their elemental composition using Energy-Dispersive X-ray Spectroscopy (EDS) and Electron Energy Loss Spectroscopy (EELS) in the Scanning Transmission Electron Microscopy (STEM) mode. Elemental maps are generated to enable elemental ultrastructural analysis of microbial cells and cells-associated mineral assemblages. Finally, there is also the possibility to detect high-resolution images of individual mineral crystalline phases. Through Fast Fourier Transformation (FFT), the lattice spacings can be measured, compared with tabulated values, and thus the various mineral phases can be characterized.

content: 1.80 mg $MnCl_2{\cdot}4H_2O$, 4.50 mg $Na_2B_4O_7{\cdot}10H_2O$, 0.22 mg $ZnSO_4{\cdot}7H_2O$, 0.05 mg $CuCl_2{\cdot}2H_2O$, 0.03 mg $Na_2MoO_4{\cdot}2\ H_2O$, 0.03 mg $VSO_4{\cdot}2\ H_2O$, and 0.01 mg $CoSO_4$ final concentration. The pH was adjusted to 2.0 with 10 N H_2SO_4. Chemolithoautotrophic cultivation was conducted at elevated temperatures (65°C and 73°C for *A. manzaensis* and *M. sedula*, respectively) as reported early (Blazevic et al., 2019; Milojevic et al., 2019a; Milojevic et al., 2021; Kölbl et al., 2022) in 0.2–1 L modified glassblower Schott-bottle bioreactors (Duran DWK Life Sciences GmbH, Wertheim/Main, Germany), supplied with a thermocouple joined to magnetic stirring and a heating plate (IKA RCT Standard/IKA C-MAG HS10, Lab Logistics Group GmbH, Meckenheim, Germany) to control agitation and temperature. The bioreactors were supplied with three 5 mL graduated glass pipettes, permitting carbon dioxide and air gassing and sampling of culture. The graduated pipettes used for gassing were connected by silicon tubing to sterile 0.2 µm filters (Millex-FG Vent filter unit, Millipore, Billerica, United States). A Luer-lock system was mounted on the sampling graduated pipettes to operate sampling with sterile syringes (Soft-Ject, Henke Sass Wolf, Tuttlingen, Germany). A water-cooled condenser (Carl Roth, Karlsruhe, Germany) was used to force the off-gas to exit. Electronic thermocouple was used to control the temperature inside the bioreactors during microbial cultivations. For chemolithoautotrophic growth, cultures were supplemented with 1–10 g/L of the mineral materials as described before (Blazevic et al., 2019; Milojevic et al., 2019a; 2021; Kölbl et al., 2022). The mineral samples were ground and temperature sterilized at 180°C in a heating chamber for a minimum of 24 h prior to autoclavation at 121°C for 20 min. Abiotic controls comprised of culture media supplemented with sterilized mineral materials, but without microbial cells, were included in all experiments. Growth of cells was observed by means of phase contrast/epifluorescence microscopy and release of soluble metal ions.

2.2 Thin sections preparation

Microbial cells were collected at stationary growth phase and primary fixed as described before (Milojevic et al., 2021) at 4°C in a 1 M Na-Cacodylate buffer supplemented with 2.5% glutaraldehyde. Followed by primary fixation, cells were post-fixed for 2 h in 1% OsO_4. After repeated washing (three times with 2 × 0.1 M Na-cacodylate, 1x dH_2O) and subsequent dehydration by a gradual ethanol series (30%, 50%, 70%, 90%, abs., each step with an incubation time of 30 min), cells were centrifuged after each dehydration step for 30 min and resuspended for the subsequent ethanol treatment. Resulting samples were embedded in Spurr Low Viscosity Resin (Electron Microscopy Sciences, United States) and polymerized at 60°C for a minimum of 48 h. Semi- and ultrathin sectioning was conducted by means of a Reichert-Jung Ultracut E ultramicrotome, with 50–70 nm ultrathin sections, followed by their staining using uranyl-acetate (15 min), and deposited on 200 copper grid mesh coated with formvar/carbon (Agar Scientific, United Kingdom).

Alternatively, sample preparation for STEM analysis has been performed by focused ion beam (FIB) sputtering as described before

(Blazevic et al., 2019; Milojevic et al., 2021) using a FEI Quanta 3D FEG instrument, equipped with an electron column hosting a field-emission electron source and an ion column hosting a Ga-liquid metal ion source (LMIS). Sputtering progress has been monitored by electron beam induced secondary electron imaging (5 keV accelerating voltage). Before sputtering, a Pt layer (length × width × height = 8 µm × 3 µm × 3 µm) was deposited onto the sample by applying FIB Pt deposition at 16 kV IB acceleration voltage. The deposited nanocrystalline Pt served as protection layer during subsequent preparation steps.

2.3 Scanning transmission electron microscopy

STEM investigations were performed on a probe-corrected FEI Titan G2 60–300 (S/TEM) microscope with an X-FEG Schottky field-emission electron source operated at 60–300 kV (current of 150 pA, beam diameter below 1 Å in STEM mode). The microscope is equipped with a Super-X detector, consisting of 4 separate silicon drift detectors (Chemi-STEM technology, Thermo Fisher Scientific) for the detection of X-ray spectra, and with a dual EELS - Gatan Imaging Filter (GIF Quantum) for the acquisition of EELS spectra. Two different high angle annular dark field (HAADF) detectors (a HAADF detector from FEI and a HAADF detector from Gatan) and an annular dark field detector (ADF), also from Gatan, were used to acquire the STEM images. The analytical investigations were performed using EDS and EELS, with a convergence angle of 19.7 mrad and a collection semiangle of 20.5 mrad (Rienks et al., 2019; Albu et al., 2016; Albu et al., 2020; Goldstein et al., 1986). Spectrum images were collected for different areas/locations of *M. sedula* cells (Milojevic et al., 2019a; Milojevic et al., 2019b; Blazevic et al., 2019). From the measured EELS and EDX spectrum images, individual EELS and EDS spectra were extracted from selected sample locations. The acquired STEM images and EELS spectra were processed via Gatan's Digital Micrograph being corrected for dark current and gain variations. EDS spectrum images were acquired and processed by using the VELOX software (Thermo Fisher Scientific).

2.4 High resolution scanning transmission electron microscopy

The high-resolution STEM (HR-STEM) micrographs of crystalline regions in different orientations to the incoming electron beam were processed by Fast Fourier Transformation (FFT) in order to measure the hkl distances. The FFT corresponds to an image of the crystallite in reciprocal space, as it also exists in the back focal plane of the objective lens in the TEM, whereby in this context we speak of electron diffraction when this plane is imaged in the TEM. The FFT of an image provides a powerful way to decompose an image into its frequency components (Williams and Carter, 2009). The interplanar distances in a certain orientation of a crystal are specific for each crystal with given lattice parameters. The Miller Indices (hkl) with the corresponding d-values are directly measured on the HRSTEM images or using the FFT images which display the frequencies spots corresponding to the inverse of the interplanar distance. The advantage of using this method is the identification of even nanocrystals of dimensions smaller than 5 nm or atomic clusters of 2–3 nm (if ordered). The FFT measured d-values (hkl) have then been compared with the possible phases extracted from the ICSD database (https://icsd.fiz-karlsruhe.de) and their calculated d-values (hkl) (Blazevic et al., 2019; Milojevic et al., 2021).

3 Results

3.1 Microbial interactions with terrestrial mineral materials

The efficient metal extracting capacities of thermoacidophilic metal oxidising microorganisms have a great potential in industrial bioleaching/biomining operations (Rawlings, 2002; Rawlings, 2005). Up to now, the metal oxidation capacity of these microorganisms has majorly been proposed as a technique in the bioprocessing of sulfide and uranium ores (Auernik and Kelly, 2010; Mukherjee et al., 2012). The tungsten–microbial interactions and microbial bioprocessing of tungsten ores are still underexplored (Milojevic, 2022). The metal mobilizing archaeon *Metallosphaera sedula* can grow on the non-sulfide tungsten ore scheelite, breaking its structure and subsequently solubilising tungsten (Blazevic et al., 2019). To investigate in depth tungsten mineral–microbial interface during scheelite biotransformation performed by *M. sedula*, we applied an integrative workflow (Figure 1), coupling electron microscopy tools and analytical nanospectroscopy. FIB milling was used to produce thin sections for high-resolution analysis of the tungsten-microbial interface in the STEM. Advanced analytical electron microscopy was used to enable ultrastructural studies of scheelite grown *M. sedula* at the nanoscale resolution (Figure 2). STEM coupled to energy-filtered transmission electron microscopy (EFTEM) analysis was used to produce the elemental maps of *M. sedula* grown on scheelite (Figures 2A–E). The elemental maps and percentage elemental composition showed tungsten biomineralization of the cell surface of *M. sedula* (Figure 2B; Supplementary Table S1). A tungsten-encrusted layer was formed around the cells of *M. sedula* with 37 ± 7 nm thickness (Supplementary Table S2). Further HR-STEM analysis revealed the W-bearing globules of irregular size that massively encrusted the S-layer of *M. sedula* cells (Figure 2G). These tungsten-bearing deposits had a crystalline microstructure with lattice parameters (Figure 2G) closely resembling various tungsten carbide structures [hexagonal WC: a = 0.28946 ± 0.01 nm, b = 0.28946 ± 0.01 nm, c = 0.28576416 ± 0.01 nm and trigonal W_2C a = 0.5188 ± 0.01 nm, b = 0.5188 ± 0.01 nm, c = 0.47273 ± 0.01 nm (Page et al., 2008; Kurlov and Gusev, 2007). Further, the EELS spectra were acquired from these tungsten globules on the cell surface layer. The EELS spectra showed the presence of a carbon K-edge at 284 eV (Figure 2I) with edge energy position and fine structure features closely resembling the carbon K-edge of a tungsten carbide (WC) reference (Blazevic et al., 2019). The similar tungsten deposits on the surface of *M. sedula* cells were also detected during cultivation with another tungsten-bearing material (Milojevic et al., 2019b). *M. sedula* was shown to decompose tungsten polyoxometalate (W-POM) clusters. When cultivated on W-POM, the surface of *M. sedula* cells was massively encrusted with W carbide-like structures that we detected by means of HR-TEM analysis

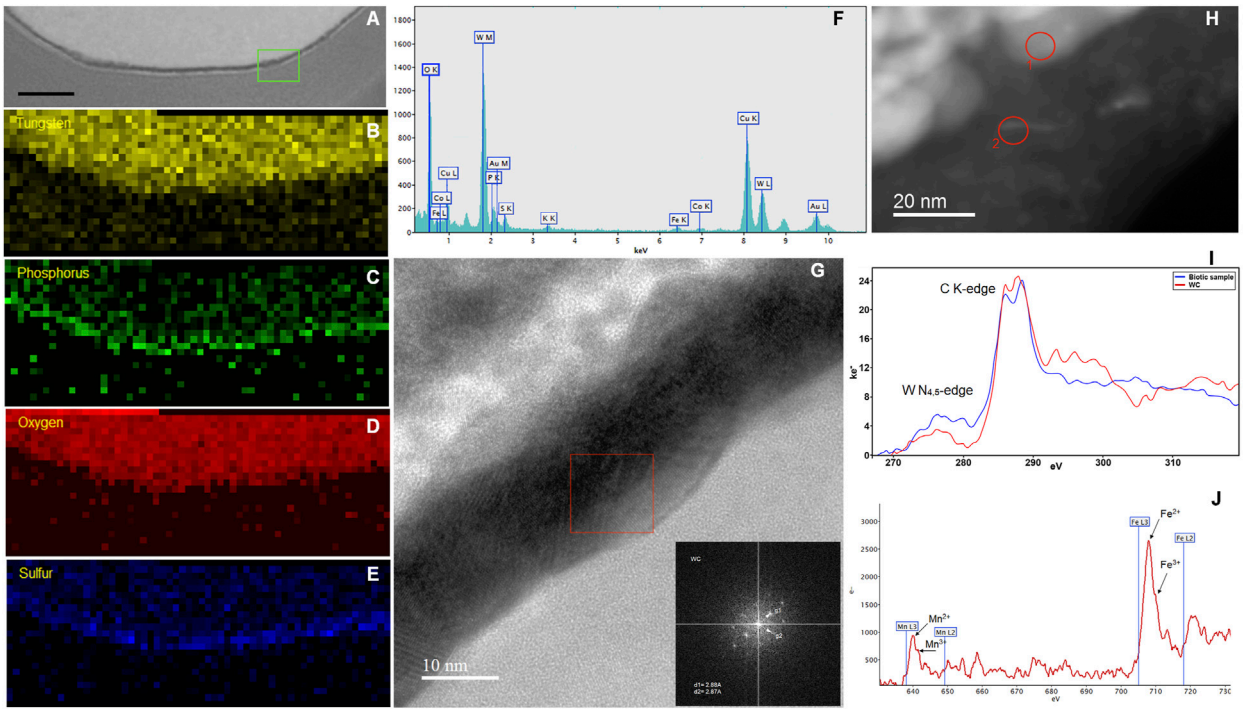

FIGURE 2
STEM based nanoanalytical spectroscopy analysis of *M. sedula* cells grown on scheelite. **(A)** Scanning transmission electron microscopy (STEM) image of a cell fragment of *M. sedula*. **(B–E)** Corresponding tungsten (W), phosphorus (P), oxygen (O), and sulfur (S) EDS elemental maps. **(F)** Energy-dispersive X-ray (EDS) spectrum acquired from the cell surface (inlet in panel **A**). Cu peaks in EDS spectra are due to the TEM grid and Au peak is due to the coating. **(G)** High-resolution STEM (HR-STEM) and Fast Fourier Transforms (FFTs) of biogenic tungsten deposits on the cell surface of *M. sedula* grown on scheelite. Inlet represents FFT acquired from the square-labeled area with tungsten crystalline cell surface deposits. **(H)** STEM image of the cell fragment of *M. sedula* used for electron energy loss spectra (EELS) analysis. **(I)** The C K-edge EEL spectra acquired from the W-encrusted cell surface layer of *M. sedula* in "1" area depicted in panel **H** and tungsten carbide reference. Modified from (Blazevic et al., 2019). **(J)** Corresponding Fe and Mn $L_{2,3}$-edge core electron energy loss (EEL) spectra acquired from "2" area depicted with circle in panel **(H)**.

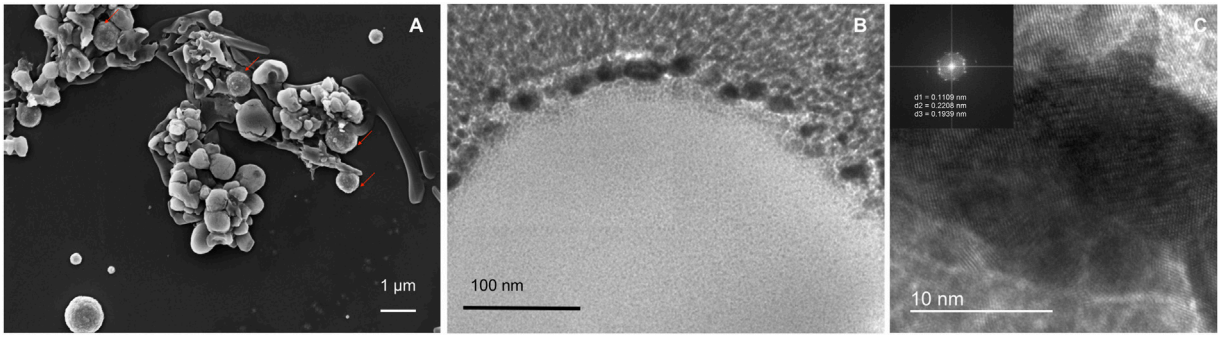

FIGURE 3
Tungsten deposits in *M. sedula* grown with tungsten polyoxometalate W-POM. Scanning Electron Microscopy (SEM) image (modified from Milojevic et al., 2019b) **(A)**, STEM image **(B)** and HR-STEM image with FFT pattern **(C)** were acquired from the tungsten crystalline deposits on cell surface. Single cells are depicted with red arrows. Inlet represents the fast fourier transform (FFT) pattern consistent with the tungsten carbide phases.

(Figure 3). Apart from this, using STEM and EELS analysis, we observed intracellular incorporation of redox heterogenous Mn- and Fe-containing nano-clusters (diameter 3–13 nm) inside *M. sedula* cells grown on scheelite (Figure 2J). The EELS spectra of these Mn-, Fe-nano-inclusions were acquired locally in STEM mode via point analysis with a beam diameter of 1 Å and showed mixed iron and manganese valences with the dominant Fe^{2+} and Mn^{2+} species (Blazevic et al., 2019).

Further investigations of the metal solubilising capacities of chemolithotrophs for bioleaching/biomining operations have shown that microbial cultures of the archaeal order Sulfolobales can extract various metals from multimetallic industrial steel waste (a secondary dust waste product of the basic oxygen furnace (BOF) steelmaking process (Gara and Schrimpf, 1998; Kölbl et al., 2022)). When grown on this metalliferous waste material, *Acidianus manzaensis* cells promote efficient metal dissolution (Kölbl et al.,

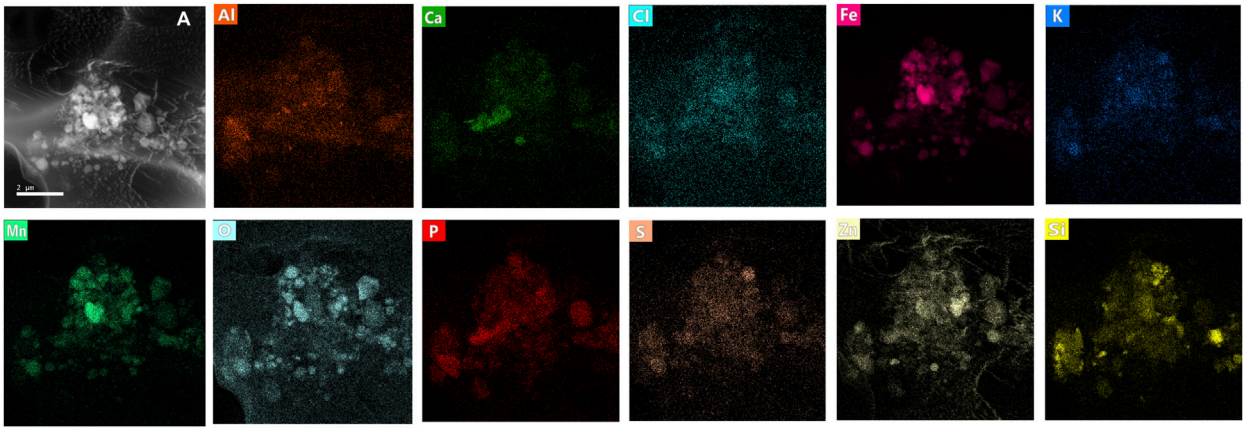

FIGURE 4
Elemental ultrastructural analysis of microbial-mineral assemblages accumulated in cultures of *A. manzaensis* grown on BOF-dust. **(A)** High angular annular dark field (HAADF-STEM) image of microbial-mineral assemblages used for the EDS spectrum image acquisition and corresponding elemental distribution maps of aluminium (Al), calcium (Ca), chlorine (Cl), iron (Fe), potassium (K), manganese (Mn), oxygen (O), phosphorus (P), sulfur (S), zinc (Zn), and silicon (Si).

2022). The efficient ability of these microorganisms to colonise and break down the mineral matrix of the metal waste product was investigated via STEM coupled to elemental analysis of the microbial-metal interfaces. For high resolution investigation, thin sections were produced via a FIB milling and examined in STEM mode. The elemental ultrastructural analysis by means of STEM-EDS demonstrated the localisation of metal and metalloid constituents of microbial-mineral assemblages formed in *A. manzaensis* cultures grown on metalliferous industrial steel waste (Figure 4; Supplementary Table S3). The elemental maps show that microbial-mineral assemblages contain P, Fe, Mn, Zn, O, S, K, Ca, Cl, Si, and Al. Single particles of BOF-dust (Figure 5) are represented by spherical grains with a diameter ranging from 2 to 80 µm (Kölbl et al., 2022) and contain all of the above elements uniformly distributed within these spheres. HR-TEM investigations also revealed another feature of spherical BOF grains, namely, a halo of nanoparticles framing their surface (Figures 5A,B). In opposite to BOF-dust spherical particles, *M. sedula* cells are coccoid morphologies around 1 µm diameter with biomineralised crust on their surface, with no halo and with void intracellular content (Figure 6). Elemental maps of Fe, Mn, P, and O closely resemble the shape of *M. sedula* cell, while Si is only partially accumulated in the cell (Figure 6). Such efficient microbial colonisation and solubilisation of various mineral matrixes should be further explored in details and applied towards various industrial mineral and metalliferous waste materials in order to develop efficient metal recovery, metal recycling processes, and waste management biotechnologies.

3.2 Microbial interactions with extraterrestrial mineral materials

Exploration of microbial-meteorite redox interactions is an essential prerequisite for the bioprocessing of extraterrestrial metal resources and the detection of microbial fingerprints (biosignatures) left on extraterrestrial mineral material. A comprehensive STEM-based analysis can provide microstructural, crystallographic, chemical, and compositional information from micrometre to sub-nanometre sized areas of microbial-meteorite interfaces. In order to explore the meteorite biogeochemistry, the extreme metallophilic thermoacidophile *M. sedula* was cultivated with H5 ordinary chondrite Northwest Africa 1172 (NWA 1172) (Russell et al., 2002; Milojevic et al., 2019a). The further analysis of the meteorite-microbial interface at nm-scale spatial resolution enabled tracing the route of meteorite inorganic constituents into a microbial cell and investigation of iron redox patterns. STEM analyses of microbial fingerprints left on NWA 1172 revealed *M. sedula* cells in different stages of biomineralization: cells with not completely mineralized cell envelope (Figure 7A) and heavily encrusted mineralized cell envelopes that correspond to advanced stages of mineral formation (Figure 7D). Elemental ultrastructural analysis via STEM-EDS showed round-shaped, irregular coccoid cellular morphologies with a diameter around 1 µm (Figure 7A) that were characterized by the abundant C, O, N, S, Cu, P, Fe, Al, Co, and K intracellular content (Milojevic et al., 2019a). In these cell, Cu, K, Cl, Fe, Al, and P signals were associated with the cell surface (Figures 7A–C). In case with heavily encrusted cell remnants, a crust layer with the thickness of 186 ± 35 nm (Supplementary Table S4) was composed of Fe, Si, Al, Ni, S, O, and P (Figures 7D,E; Supplementary Table S5). Further comparative electron energy loss spectra (EELS) analysis demonstrated the fine structure of iron species in heavily encrusted cell remnants and on the cell surface of *M. sedula* (Figure 7F). The EELS measurements were performed in STEM mode and were acquired locally by point analysis with a beam diameter of 1 Å. These EELS measurements demonstrate a mixed valence iron distribution with dominant Fe^{2+} species at the cell surface of *M. sedula* (red line at Figure 7F, Fe $L_{2,3}$-edge at −708 eV). The Fe $L_{2,3}$-edges from heavily encrusted cell envelops are characterised by the predominant presence of Fe^{3+} species (violet line at Figure 7F, Fe $L_{2,3}$-edge at −710 eV), which can be explained by accomplished Fe^{2+} oxidation followed by cell encrustation and entombment in the mineralized form of a mixture of different amorphous iron oxides/hydroxides with the predominant form of Fe^{3+} (Milojevic et al., 2019a).

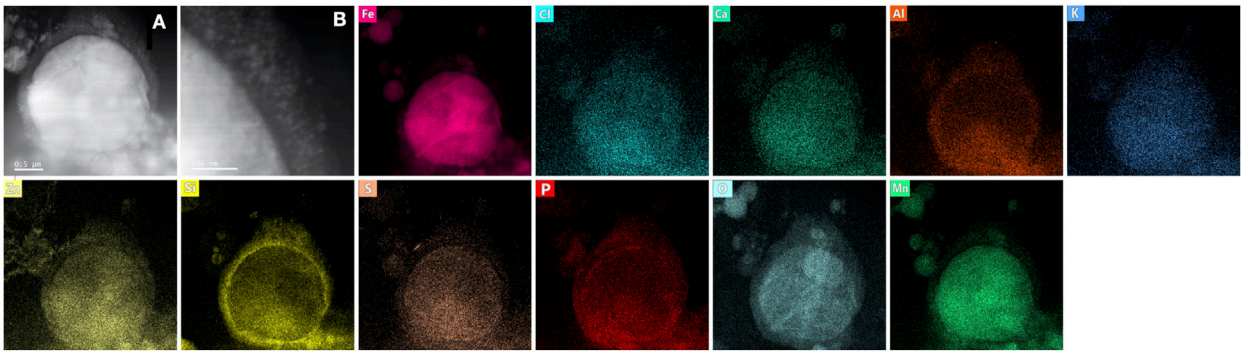

FIGURE 5
(A, B) HAADF-STEM images of a single BOF-dust particle used for the EDS spectrum image acquisition and corresponding elemental distribution maps of iron (Fe), chlorine (Cl), calcium (Ca), aluminium (Al), potassium (K), zinc (Zn), silicon (Si), sulfur (S), phosphorus (P), oxygen (O), and manganese (Mn).

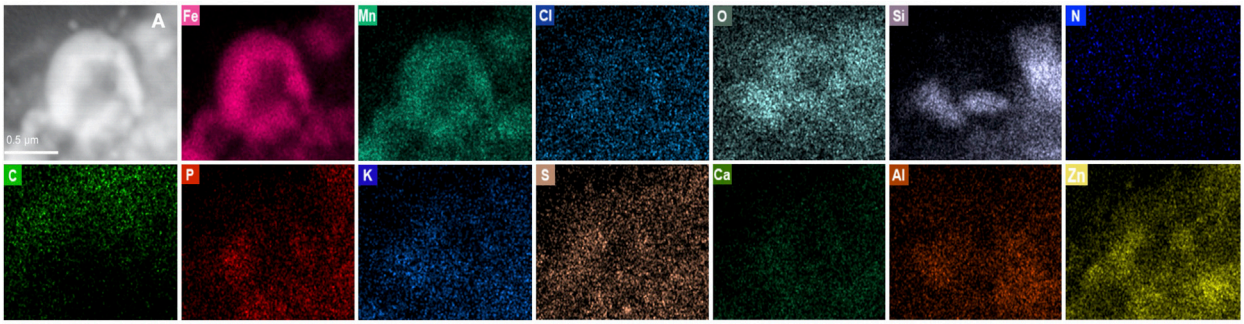

FIGURE 6
Elemental ultrastructural analysis of *A. manzaensis* single cell grown on BOF-dust. **(A)** The HAADF-STEM image of a microbially processed sample used for the EDS spectrum image acquisition and corresponding elemental distribution maps of iron (Fe), manganese (Mn), chlorine (Cl), oxygen (O), silicon (Si), nitrogen (N), carbon (C), phosphorus (P), potassium (K), sulfur (S), calcium (Ca), aluminium (Al), and zinc (Zn). Modified from (Kölbl et al., 2022).

To address Mars-relevant biosignatures, the extreme metallophilic thermoacidophile *M. sedula* was grown on the genuine Noachian Martian breccia Northwest Africa (NWA) 7,034 (Nyquist, 2016; Cassata et al., 2018) and the resulting microbial–meteorite interactions were investigated at the nanometer scale (Milojevic et al., 2021). Elemental ultrastructural analysis of *M. sedula* grown on NWA 7,034 by using EELS (Figures 8A–E) and EDS (Figure 8H; Supplementary Table S6) in STEM mode showed that the cells are encrusted in an Fe-, Mn-, Al-, and P-bearing layer of 28 ± 2 nm thickness (Figure 8F; Supplementary Table S7). As shown further by HR-STEM analysis, this encrusted outer layer has a crystalline microstructure with lattice parameters closely resembling different phosphate assemblages: Fe/Mn phosphates (hkl-d-value 0.154 ± 0.01 nm) and Al phosphates (hkl-d-value 0.412 ± 0.01 nm) (Figure 8F, inlet) (Milojevic et al., 2021). Cells at the early stages of biomineralization showed the accumulation of the nanometer-sized near-spherical aggregates, mainly composed of Fe, O, Si, and Mn as shown by STEM- EDS analysis (Figure 8G). These amorphous nanoassemblages were converted at the late biomineralization stages into Fe- and Mn-bearing intracellular crystalline deposits of a very complex and heterogeneous nature (Milojevic et al., 2021).

4 Discussion and conclusion

Mineral and metal processing microorganisms play important roles in environmental history, redox cycling of elements, shaping of rock records, and formation of ore deposits. Microbial-mineral interactions have been harnessed in biomining operations, exploited in sustainable green biotechnologies, and considered as important sources of mineral biosignatures for studying early life on Earth and beyond. Resolving microbial-mineral interfaces is crucial to our understanding of the transition from mineral geochemistry to biochemistry of a living organism. Investigating microbial bioprocessing of tungsten ores, the nanolayers of tungsten carbide-like material deposited over the microbial cell surface were described and its physicochemical characterization was reported using a comprehensive set of STEM based techniques (Figures 2, 3). These biogenic cell surface tungsten carbide-like nanostructures could be used as a potential sustainable nanomaterial obtained by environmentally friendly microbial biotechnologies. Furthermore, these results indicated that *M. sedula* forms tungsten-bearing mineralized cell surface via encrusting with tungsten carbide-like compounds. Tungsten-encrusted layer represents a microbial strategy to withstand harsh

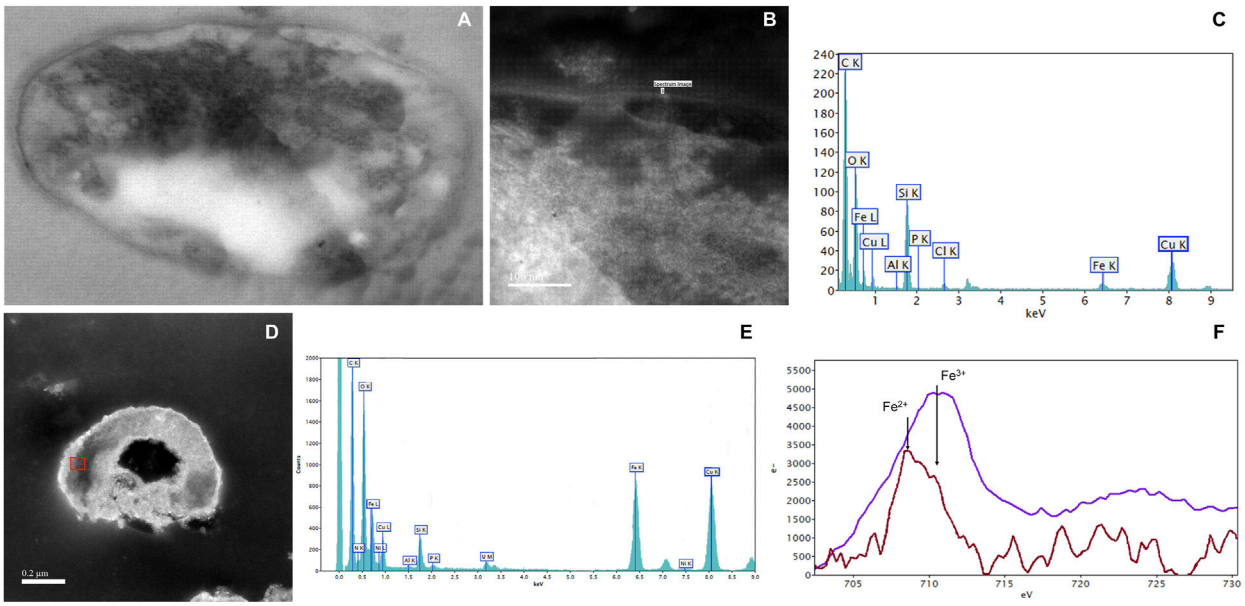

FIGURE 7
Nanoanalytical spectroscopy of microbial-meteorite NWA 1172 interface. **(A)** The HAADF-STEM image of a cell of *M. sedula* used for the EDS spectrum image acquisition. **(B)** The annular dark field (ADF) STEM image of a cell fragment of *M. sedula* used for the EDS spectrum image acquisition. **(C)** EDS spectra acquired from the cell surface area depicted in panel **(B)**. **(D)** The HAADF image of a heavily encrusted remnants of *M. sedula* cell used for the EDS spectrum acquisition. **(E)** EDS spectra acquired from the surface area depicted in panel **(D)**. **(F)** Corresponding Fe $L_{2,3}$-edge core electron energy loss (EEL) spectra acquired from the surface area of *M. sedula* cell depicted in B (shown as red line) and from the crust remnants depicted in D (shown as violet line). **(D,F)** Modified from (Milojevic et al., 2019a).

environments (Kölbl et al., 2020), such as during an interplanetary journey. The observed tungsten encapsulation can serve as a potent radioprotective armour against drastic environments, enabling our study of microbial survivability in outer space environment (Kölbl et al., 2020). The phenomenon of tungsten encapsulation can be connected to the highly ordered proteinaceous S-layer of *M. sedula* which facilitated the sorption of the metal ions serving as nucleation centres for further crystallization and this way promoting the nanoparticles growth. Importantly, we have reported the redox heterogenous intracellular inclusions of Mn and Fe during the scheelite biotransformation (Figure 2J). The analysis of scheelite chemical composition have shown impurities of Mn and Fe oxides (0.2% and 19.0% w/w, correspondingly) (Blazevic et al., 2019). These Mn and Fe trace impurities in scheelite most likely served as an origin of the observed Mn, Fe-bearing intracellular nano-inclusions. The reported intracellular inclusions with iron and manganese in mixed valence states may represent a nanometer sized energy storage depot for *M. sedula* cells, functioning as clusters of metal ions with redox potential appropriate for biooxidative metabolic activity of *M. sedula*. Such Fe, Mn-bearing nano-inclusions could potentially provide reduced metallic species (Fe^{2+} and Mn^{2+}) deposited inside the cell as a storage depot, which may be used by *M. sedula* to satisfy energy demand for its respiration needs. This assumption, however, requires further thorough investigations to understand the correlation of these intracellular Fe and Mn inclusions with the biooxidation activity of *M. sedula* and to identify the actual energy sources for growth on scheelite. It is possible to propose that along with abiotic chemical factors, the microbially mediated biooxidation of iron and manganese destroyed the scheelite structure, leading to mineral breakage and the release of W into solution (Blazevic et al., 2019). These results obtained using the STEM-based approach are useful for understanding the mechanism of microbial biotransformation of scheelite and expanding our knowledge of the currently underrepresented and less studied biomining of tungsten ores.

Using STEM based set of techniques, a great potential of thermoacidophilic metal oxidising microorganisms has been further investigated for biomining/bioleaching operations that are based on their efficient metal solubilising capacities. It has been recently shown that such microbial cultures can extract various metals from multimetallic industrial steel waste, promoting efficient metal dissolution and improving bioleaching performance (Kölbl et al., 2022; Memic et al., 2024). The efficient ability of microorganisms to interact with, colonise and break down the mineral matrix of the metal waste product was observed via STEM based approach (Figures 4–6). These investigations promoted our understanding of metal extraction capacities of these microorganisms and facilitated the design of microbial consortia (Memic et al., 2024; Kölbl et al., 2023) to break down solid matrix of metalliferous waste for metal recycling processes in frames of circular economies.

Owing to its high spatial resolution and comprehensive analytical capacities, STEM based nanospectroscopy has been successfully applied to extend our knowledge of meteorite biogeochemistry and resolve microbial interfaces with astromaterials (Milojevic et al., 2019a; Milojevic et al., 2021). Among astrobiological implications of microbial-mineral interactions are biosignatures as putative evidence of past habitability on planetary bodies (Westall et all., 2015), as well as biomining of asteroid materials in frames of *in situ* resource

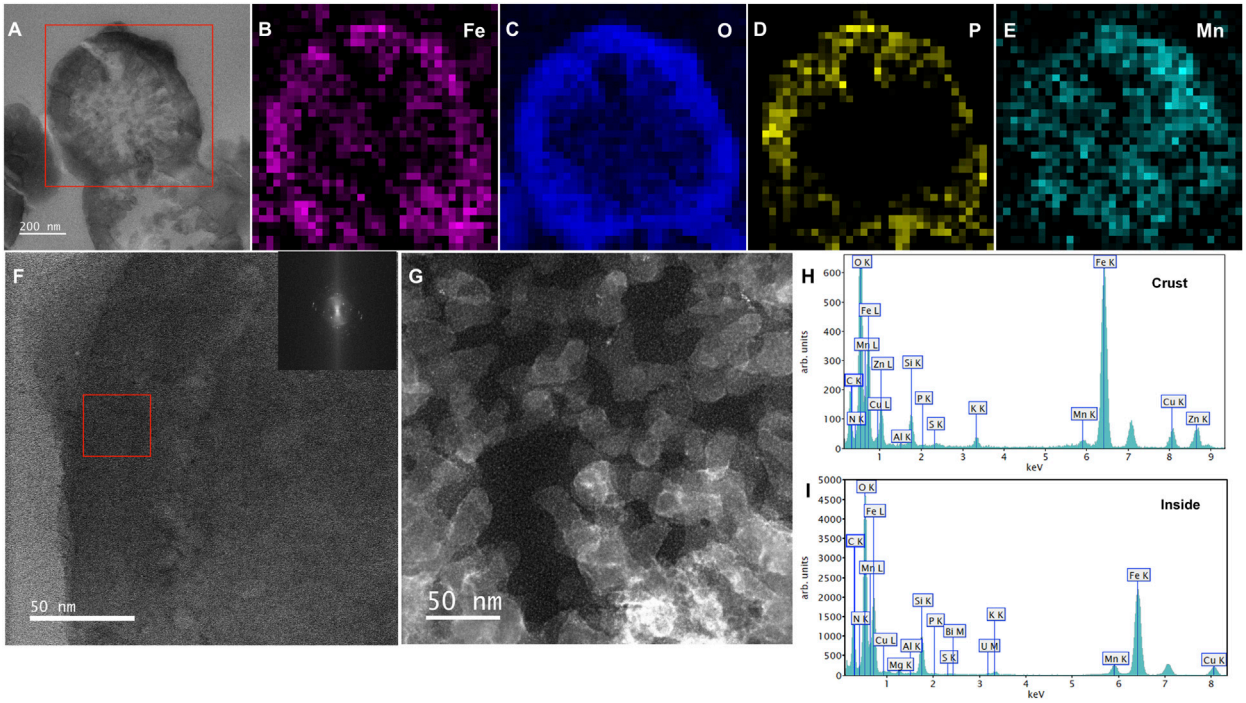

FIGURE 8
Nanoanalytical spectroscopy analyses of *M. sedula* cells grown on the Noachian Martian breccia NWA 7034. **(A)** The HAADF-STEM image of *M. sedula* cells used for the EELS spectrum image acquisition. **(B–E)** Representative iron (Fe), oxygen (O), phosphorus (P), and manganese (Mn) elemental maps extracted from the area depicted in red square in **(A)**. **(F)** Representative HR-STEM image of biogenic mineral deposits in the outer crust of *M. sedula* cell. Inlet represents the FFT pattern acquired from the area depicted in red square, which is consistent with the phases of Fe, Mn, Al phosphates (Milojevic et al., 2021). **(G)** The HR-STEM image of the intracellular amorphous nanoassemblages in *M. sedula* cell. **(H)** EDS spectra acquired from the outer crust of *M. sedula* cell depicted in panel **(F)**. **(I)** EDS spectra acquired from the nanometer-sized near-spherical aggregates in panel **(G)**.

utilization (ISRU) programs (Santomartino et al., 2023). The biogeochemical fingerprints left upon microbial growth on the NWA 1172 meteorite were examined via a combination of several analytical nanospectroscopy techniques with STEM imaging (Milojevic et al., 2019a). Redox heterogeneous iron species Fe^{2+}/Fe^{3+} with dominant Fe^{2+} on the microbial cell surface (Figure 7) point to an active Fe redox processing and suggest Fe biooxidative solubilization of meteorite material. Cells of *M. sedula* incorporate various metals when grown on this meteorite material (Figure 7). They form heavily metal encrusted cell remnants with fine structural details (Milojevic et al., 2019a) that may constitute mineral biosignatures, if they persist diagenetic or metamorphic processes and remain preserved during different stages of fossilization. These investigations demonstrated the enrichment of Cu, Fe, O, and Si in the microbial crust with a mixture of P, Ni, S and Al, which may likely correspond to the amorphous product $Cu_xFe_yO_z$ (SPNiAl)–SiO_2 (Milojevic et al., 2019a) formed on the late stages of cells encrustation (Figures 7D,E).

Biosignatures as key evidence for the existence of biological entities are of particular importance in the search for life in the Mars rock record. The current Mars rovers are specifically equipped to search for possible ancient biosignatures on Mars. If life ever arose and spread on Mars, the traces of fossil evidence of the earliest Martian biosphere may be well accessible in subsurface sediments (McKay and Stoker, 1989; Malin and Edgett, 2000; Grotzinger and Milliken, 2012; Westall et al., 2015; Hays et al., 2017). The possible origin and fingerprints of microbial activity and metabolism on Mars may be detected in rock records using microfossil remnants (Cavalazzi et al., 2021), biomarkers (Baqué et al., 2022), and other molecular biosignatures derived from living systems (Summons et al., 2007). We have recently conducted experiments on microbially assisted chemolithotrophy based on Martian genuine meteorite NWA 7034 (Milojevic et al., 2021). The recent study on this Noachian Martian breccia composed of ~4.5 Gyr old crustal materials from Mars, delivered a prototype of microbial life laboratory designed on a real Martian mineral material. These experiments provided a possibility to investigate the putative bioalteration processes of the Martian crust. The STEM based investigations of this prototype of Martian life (Milojevic et al., 2021) delivered a rich source of Mars relevant mineral and metabolic biosignatures, which may promote future nano-assessment of the biogenicity of returned Mars samples. Assessing the fine-scale heterogeneity of microbial-NWA 7034 interface, we have noticed that the biomineralization patterns of *M. sedula* grown on genuine Martian material differ substantially from the biomineralization patterns of the same microorganism grown on ordinary chondrite NWA 1172 (Milojevic et al., 2019a) and terrestrial minerals (Blazevic et al., 2019; Milojevic et al., 2019b; Usher et al., 2009). These observations are in line with the statement that the mineralogical environmental settings dictate biomineralisation patterns and likely preservation potential of chemolithotrophs. Encapsulation with a thick Fe(Mn, Al)/P-outer layer with P solely represented in this layer (Figure 8) and intracellular crystalline Fe/Mn oxides and Mn silicates (Milojevic

et al., 2021) are distinguishable features of the growth on the Noachian Martian breccia NWA 7034. This drastic difference of the biomineralization patterns emphasizes the importance of experiments on genuine Martian materials for Mars-relevant astrobiological investigations. The phosphate-rich content of the NWA 7034 could be a source of phosphates in the outer crust of *M. sedula* cell. Further investigations with Mars mineral analogues may help understanding the influence of abiotic factors on microbial biomineralisation patterns. The densely $Fe_nMn_xAl_yP_z$-encapsulated cells (Figure 8) with intracellular crystalline deposits (Fe_3O_4/Mn_3O_4/$Mn_xSi_yO_z$) may form relevant putative biosignatures to be searched in the Martian rock record, if they withstand destructive environmental constrains. The nanoscale microbial-mineral interfaces of chemolithotrophs grown on Mars genuine meteorites should be further thoroughly investigated with various spectroscopic techniques. These investigations are important as a guiding point for *in situ* analyse of collected Mars samples.

The presented results feature unique metallophilic life in hostile environments, extending knowledge of the geobiochemistry of microbial-mineral interactions. Based on these findings, obtained via STEM based nanoanalytical approach, biohydrometallurgical processing of mineral ores and metallic waste materials can be further improved. Importantly, biogenic alteration of Martian mineral materials explored via STEM based nanoanalysis is a potential source of Mars-relevant biosignatures for astrobiological investigations in light of life search missions. Further development of the sample preparation techniques including cryo-assisted methodologies to investigate fragile and brittle geomicrobiological samples via STEM based approach would be necessary to increase reproducibility of the measurements.

Data availability statement

The original contributions presented in the study are included in the article/Supplementary Material, further inquiries can be directed to the corresponding author.

Author contributions

TM: Conceptualization, Data curation, Formal Analysis, Funding acquisition, Investigation, Methodology, Project administration, Resources, Supervision, Validation, Visualization, Writing – original draft, Writing – review and editing. MA: Data curation, Formal Analysis, Investigation, Methodology, Software, Validation, Visualization, Writing – review and editing. IL-P: Data curation, Formal Analysis, Resources, Software, Visualization, Writing – review and editing. AM: Visualization, Software, Writing – original draft, Writing – review and editing.

Funding

The author(s) declare that financial support was received for the research and/or publication of this article. This research was funded by European Research Council, grant number ERC-2020-COG-ERC, CONSOLIDATOR GRANT 101001311, the French National Research Agency (ANR, CPJ n°ANR-22-CPJ1-0066-01) and the Austrian Science Foundation (FWF Elise-Richter Research fellowship V333) to TM.

Acknowledgments

We warmly thank S. Puchegger (University of Vienna, Physics Faculty Centre for Nanostructure Research) for the support in the electron microscopy investigations and Claudia Mayrhofer (FELMI, Graz) for the help with thin sections preparation.

Conflict of interest

The authors declare that the research was conducted in the absence of any commercial or financial relationships that could be construed as a potential conflict of interest.

The author(s) declared that they were an editorial board member of Frontiers, at the time of submission. This had no impact on the peer review process and the final decision.

Generative AI statement

The author(s) declare that no Generative AI was used in the creation of this manuscript.

Publisher's note

All claims expressed in this article are solely those of the authors and do not necessarily represent those of their affiliated organizations, or those of the publisher, the editors and the reviewers. Any product that may be evaluated in this article, or claim that may be made by its manufacturer, is not guaranteed or endorsed by the publisher.

Supplementary material

The Supplementary Material for this article can be found online at: https://www.frontiersin.org/articles/10.3389/fenvc.2025.1581103/full#supplementary-material

References

Albu, M., Fitzek, H., Moser, D., Kothleitner, G., and Hofer, F. (2020). Multiscale and correlative analytical electron microscopy of extraterrestrial minerals. *Front. Astron. Space Sci.* 7, 544331. doi:10.3389/fspas.2020.544331

Albu, M., Pal, A., Gspan, C., Picu, R. C., Hofer, F., and Kothleitner, G. (2016). Self-organized Sr leads to solid state twinning in nano-scaled eutectic Si phase. *Sci. Rep.* 6, 31635. doi:10.1038/srep31635

Auernik, K. S., Cooper, C. R., and Kelly, R. M. (2008). Life in hot acid: pathway analyses in extremely thermoacidophilic archaea. *Curr. Opin. Biotechnol.* 5, 445–453. doi:10.1016/j.copbio.2008.08.001

Auernik, K. S., and Kelly, R. M. (2010). Physiological versatility of the extremely thermoacidophilic archaeon Metallosphaera sedula supported by transcriptomic analysis of heterotrophic, autotrophic, and mixotrophic growth. *Front. Microbiol.* 76, 931–935. doi:10.1128/AEM.01336-09

Banerjee, I., Burrell, B., Reed, C., West, A. C., and Banta, S. (2017). Metals and minerals as a biotechnology feedstock: engineering biomining microbiology for bioenergy applications. *Curr. Opin. Biotech.* 45, 144–155. doi:10.1016/j.copbio.2017.03.009

Baqué, M., Backhaus, T., Meeßen, J., Hanke, F., Böttger, U., Ramkissoon, N., et al. (2022). Biosignature stability in space enables their use for life detection on Mars. *Sci. Adv.* 8, eabn7412. doi:10.1126/sciadv.abn7412

Blazevic, A., Albu, M., Mitsche, S., Gerlinde, H., and Milojevic, T. (2019). Biotransformation of scheelite CaWO4 by the extreme thermoacidophile Metallosphaera sedula: tungsten-microbial interface. *Front. Microbiol.* 10, 1492. doi:10.3389/fmicb.2019.01492

Bosecker, K. (1997). Bioleaching: metal solubilization by microorganisms. *FEMS Microbiol. Rev.* 20, 591–604. doi:10.1111/j.1574-6976.1997.tb00340.x

Bristow, T. F., Bish, D. L., Vaniman, D. T., Morris, R. V., Blake, D. F., Grotzinger, J. P., et al. (2015). The origin and implications of clay minerals from Yellowknife Bay, Gale crater, Mars. *Am. Mineral.* 100, 824–836. doi:10.2138/am-2015-5077ccbyncnd

Camprubi, E., Jordan, S. F., Vasiliadou, R., and Lane, N. (2017). Iron catalysis at the origin of life. *IUBMB Life* 69, 373–381. doi:10.1002/iub.1632

Cassata, W. S., Cohen, B. E., Mark, D. F., Trappitsch, R., Carolyn, A., Wimpenny, J., et al. (2018). Chronology of Martian breccia NWA 7034 and the formation of the Martian crustal dichotomy. *Sci. Adv.* 4, eaap8306. doi:10.1126/sciadv.aap8306

Cavalazzi, C., Lemelle, L., Simionovici, A., Cady, S. L., Russell, M. J., Bailo, E., et al. (2021). Cellular remains in a ~3.42-billion-year-old subseafloor hydrothermal environment. *Sci. Adv.* 7, eabf3963. doi:10.1126/sciadv.abf3963

Claassens, N., Sousa, D. Z., dos Santos, V. A. P. M., de Vos, W. M., and van der Oost, J. (2016). Harnessing the power of microbial autotrophy. *Nat. Rev. Microbiol.* 14, 692–706. doi:10.1038/nrmicro.2016.130

Farquhar, J., Savarino, J., Jackson, T. L., and Thiemens, M. H. (2000). Evidence of atmospheric sulphur in the Martian regolith from sulphur isotopes in meteorites. *Nature* 404, 50–52. doi:10.1038/35003517

Gara, S., and Schrimpf, S. (1998). Behandlung von Reststoffen und Abfällen in der Eisen- und Stahlindustrie. Wien: Bundesministerium für Umwelt, Jugend und Familie.

Giachino, A., Focarelli, F., Marles-Wright, J., and Waldron, K. J. (2021). Synthetic biology approaches to copper remediation: bioleaching, accumulation and recycling. *FEMS Microbiol. Ecol.* 97, 249. doi:10.1093/femsec/fiaa249

Goldstein, J. I., Williams, D. B., and Cliff, G. (1986). "Quantification of energy dispersive spectra," in *Principles of analytical electron microscopy*. Editors D. C. Joy, A. D. Romig, and J. L. Goldstein, 155–217.

Grotzinger, J. P., and Milliken, R. E. (2012). "The sedimentary rock record of Mars: distribution, origins, and global stratigraphy," in *Sedimentary geology of Mars*. Editors J. P. Grotzinger, and R. E. Milliken, 1–48.

Grotzinger, J. P., Sumner, D. Y., Kah, L. C., Stack, K., Gupta, S., Edgar, L., et al. (2014). A habitable fluvio-lacustrine environment at Yellowknife Bay, Gale crater, Mars. *Science* 343, 1242777. doi:10.1126/science.1242777

Hays, L. E., Graham, H. V., Des Marais, D. J., Hausrath, E. M., Horgan, B., McCollom, T. M., et al. (2017). Biosignature preservation and detection in Mars analog environments. *Astrobiology* 17, 363–400. doi:10.1089/ast.2016.1627

Huber, G., Spinnler, C., Gambacorta, A., and Stetter, K. O. (1989). Metallosphaera sedula gen. and sp. nov. represents a new genus of aerobic, metal-mobilizing, thermoacidophilic Archaebacteria. *Syst. Appl. Microbiol.* 12, 38–47. doi:10.1016/s0723-2020(89)80038-4

Hurowitz, J. A., Grotzinger, J. P., Fischer, W. W., McLennan, S. M., Milliken, R. E., Stein, N., et al. (2017). Redox stratification of an ancient lake in Gale crater, Mars. *Science* 356, eaah6849. doi:10.1126/science.aah6849

Kölbl, D., Blazevic, A., Albu, M., Fasching, C., and Milojevic, T. (2020). Desiccation of the Extreme Thermoacidophile Metallosphaera sedula Grown on Terrestrial and Extraterrestrial Materials. *Front. Astron. Space Sci.* 7, 4. doi:10.3389/fspas.2020.00041

Kölbl, D., Memic, A., Schnideritsch, H., Wohlmuth, D., Klösch, G., Albu, M., et al. (2022). Thermoacidophilic bioleaching of industrial metallic steel waste product. *Front. Microbiol.* 13, 864411. doi:10.3389/fmicb.2022.864411

Kölbl, D., Memic, A., Schnideritsch, H., Wohlmuth, D., Klösch, G., Albu, M., et al. (2023). Bacterial metal accumulation as a strategy for waste recycling management. *Resources* 12, 144. doi:10.3390/resources12120144

Konhauser, K. O., Lalonde, S. V., Planavsky, N. J., Pecoits, E., Lyons, T. W., Mojzsis, S. J., et al. (2011). Aerobic bacterial pyrite oxidation and acid rock drainage during the Great Oxidation Event. *Nature* 478 (7369), 369–373. doi:10.1038/nature10511

Krebs, W., Brombacher, C., Bosshard, P. P., Bachofen, R., and Brandl, H. (1997). Microbial recovery of metals from solids. *FEMS Microbiol. Rev.* 20, 605–617. doi:10.1016/s0168-6445(97)00037-5

Kurlov, A. S., and Gusev, A. I. (2007). Neutron and x-ray diffraction study and symmetry analysis of phase transformations in lower tungsten carbide W2C. *Phys. Rev. B.* 76, 174115. doi:10.1103/PhysRevB.76.174115

Malin, M. C., and Edgett, K. S. (2000). Sedimentary rocks of early Mars. *Science* 290, 1927–1937. doi:10.1126/science.290.5498.1927

McKay, C. P., and Stoker, C. R. (1989). The early environment and its evolution on Mars: implication for life. *Rev. Geophys.* 2, 189–214. doi:10.1029/rg027i002p00189

Memic, A., Mashchenko, A., Kölbi, D., Schnideritsch, H., Wohlmuth, D., Klösch, G., et al. (2024). Bioleaching of industrial metallic steel waste by mixed cultures of thermoacidophilic archaea. *Processes* 12, 2327. doi:10.3390/pr12112327

Milojevic, T. (2022). "Microbial tungsten assimilation," in *Microbial metabolism of metals and metalloids*. Editor C. J. Hurst (Springer). doi:10.1007/978-3-030-97185-4

Milojevic, T., Albu, M., Blazevic, A., Gumerova, N., Konrad, L., and Cyran, N. (2019b). Nanoscale tungsten-microbial interface of the metal immobilizing thermoacidophilic archaeon Metallosphaera sedula cultivated with tungsten polyoxometalate. *Front. Microbiol.* 10, 1267. doi:10.3389/fmicb.2019.01267

Milojevic, T., Albu, M., Kölbl, D., Kothleitner, G., Bruner, R., and Morgan, M. L. (2021). Chemolithotrophy on the Noachian Martian breccia NWA 7034 via experimental microbial biotransformation. *Commun. Earth Environ.* 2, 39. doi:10.1038/s43247-021-00105-x

Milojevic, T., Kölbl, D., Ferrièrem, L., Albu, M., Kish, A., Flemming, R. L., et al. (2019a). Exploring the microbial biotransformation of extraterrestrial material on nanometer scale. *Sci. Rep.* 9, 18028. doi:10.1038/s41598-019-54482-7

Morrison, P. R., and Mojzsis, S. J. (2020). Tracing the early emergence of microbial sulfur metabolisms. *Geomicrobiol. J.* 38, 66–86. doi:10.1080/01490451.2020.1812773

Mukherjee, A., Wheaton, G. H., Blum, P. H., and Kelly, R. M. (2012). Uranium extremophily is an adaptive, rather than intrinsic, feature for extremely thermoacidophilic metallosphaera species. *Proc. Natl. Acad. Sci. U. S. A.* 109, 16702–16707. doi:10.1073/pnas.1210904109

Nyquist, L. E., Shih, C., McCubbin, F. M., Santos, A. R., Shearer, C. K., Peng, Z. X., et al. (2016). Rb-Sr and Sm-Nd isotopic and REE studies of igneous components in the bulk matrix domain of Martian breccia Northwest Africa 7034. *Meteorit. Planet. Sci.* 51, 483–498. doi:10.1111/maps.12606

Page, K., Li, J., Savinelli, R., Szumila, H. N., Zhang, J., Stalick, J. K., et al. (2008). Reciprocal-space and real-space neutron investigation of nanostructured Mo2C and WC. *Solid State Sci.* 10, 1499–1510. doi:10.1016/j.solidstatesciences.2008.03.018

Pham, V. H. T., Kim, J., Chang, S., and Chung, W. (2022). Bacterial biosorbents, an efficient heavy metals green clean-up strategy: prospects, challenges, and opportunities. *Microorganisms* 10, 610. doi:10.3390/microorganisms10030610

Rawlings, D. E. (2002). Heavy metal mining using microbes. *Annu. Rev. Microbiol.* 56, 65–91. doi:10.1146/annurev.micro.56.012302.161052

Rawlings, D. E. (2005). Characteristics and adaptability of iron- and sulfur-oxidizing microorganisms used for the recovery of metals from minerals and their concentrates. *Microb. Cell Fact.* 4, 13. doi:10.1186/1475-2859-4-13

Rienks, E. D. L., Wimmer, S., Sánchez-Barriga, J., Caha, O., Mandal, P. S., Růžička, J., et al. (2019). Large magnetic gap at the Dirac point in Bi2Te3/MnBi2Te4 heterostructures. *Nature* 576, 423–428. doi:10.1038/s41586-019-1826-7

Russell, S., Zipfel, J., Grossman, J., and Grady, M. (2002). The Meteoritical Bulletin No. 86. Meteorit. *Planet. Sci.* 37, 157–184.

Santomartino, R., Averesch, N. J. H., Bhuiyan, M., Cockell, C. S., Colangelo, J., Gumulya, Y., et al. (2023). Toward sustainable space exploration: a roadmap for harnessing the power of microorganisms. *Nat. Commun.* 14 (1), 1391. doi:10.1038/s41467-023-37070-2

Schippers, A., Hedrich, S., Vasters, J., Drobe, M., Sand, W., and Willscher, S. (2013). in *Biomining: metal recovery from ores with microorganisms*. Editors I. Geobiotechnology, A. Schippers, F. Glombitza, and W. Sand (Berlin, Heidelberg: Springer Berlin Heidelberg), 1–47. doi:10.1007/10_2013_216

Summons, R. E., Albrecht, P., McDonald, G., and Moldowan, J. M. (2007). Molecular biosignatures. *Space Sci. Rev.* 135, 133–159. doi:10.1007/s11214-007-9256-5

Usher, K. M., Shaw, J. A., Plumb, J. J., and Saunders, M. (2009). Elemental ultrastructure of bioleaching bacteria and archaea grown on different energy sources. *Adv. Mater. Res.* 71, 235–238. doi:10.4028/www.scientific.net/AMR.71-73.235

Vaniman, D. T., Bish, D. L., Ming, D. W., Bristow, T. F., Morris, R. V., Blake, D. F., et al. (2014). Mineralogy of a mudstone at yellowknife bay, gale crater, Mars. *Science* 343, 1243480. doi:10.1126/science.1243480

Wächtershäuser, G. (1988). Pyrite formation, the first energy source for life: a hypothesis. *Syst. Appl. Microbiol.* 10, 207–210. doi:10.1016/s0723-2020(88)80001-8

Wächtershäuser, G. (1990). Evolution of the first metabolic cycles. *Proc. Natl. Acad. Sci. U. S. A.* 87, 200–204. doi:10.1073/pnas.87.1.200

Weiss, M. C., Weiss, M. C., Sousa, F. L., Mrnjavac, N., Neukirchen, S., Roettger, M., et al. (2016). The physiology and habitat of the last universal common ancestor. *Nat. Microbiol.* 1, 16116. doi:10.1038/nmicrobiol.2016.116

Westall, F., Foucher, F., Bost, N., Bertrand, M., Loizeau, D., Vago, J. L., et al. (2015). Biosignatures on Mars: what, where, and how? Implications for the search for martian life. *Astrobiology* 15 (11), 998–1029. doi:10.1089/ast.2015.1374

Williams, D. B., and Carter, C. B. (2009). "High-resolution TEM: a textbook for materials science," in *Band 1*. Springer Science and Business Media.

Yoshida, N., Nakasato, M., Ohmura, N., Ando, A., Saiki, H., Ishii, M., et al. (2006). Acidianus manzaensis sp. nov., a novel thermoacidophilic archaeon growing autotrophically by the oxidation of H2 with the reduction of Fe3+. *Curr. Microbiol.* 53, 406–411. doi:10.1007/s00284-006-0151-1